



HAL
open science

A Class of Nonlocal Variational Problems on a Vector Bundle for Color Image Local Contrast Reduction/Enhancement.

Thomas Batard, Marcelo Bertalmío

► **To cite this version:**

Thomas Batard, Marcelo Bertalmío. A Class of Nonlocal Variational Problems on a Vector Bundle for Color Image Local Contrast Reduction/Enhancement. . 2015. hal-01202922v1

HAL Id: hal-01202922

<https://hal.science/hal-01202922v1>

Preprint submitted on 21 Sep 2015 (v1), last revised 19 Feb 2016 (v2)

HAL is a multi-disciplinary open access archive for the deposit and dissemination of scientific research documents, whether they are published or not. The documents may come from teaching and research institutions in France or abroad, or from public or private research centers.

L'archive ouverte pluridisciplinaire **HAL**, est destinée au dépôt et à la diffusion de documents scientifiques de niveau recherche, publiés ou non, émanant des établissements d'enseignement et de recherche français ou étrangers, des laboratoires publics ou privés.

A Class of Nonlocal Variational Problems on a Vector Bundle for Color Image Local Contrast Reduction/Enhancement. *

Thomas Batard and Marcelo Bertalmío

Abstract: We extend two existing variational models from the Euclidean space to a vector bundle over a Riemannian manifold. The Euclidean models, dedicated to regularize or enhance some color image features, are based on the concept of nonlocal gradient operator acting on a function of the Euclidean space. We then extend these models by generalizing this operator to a vector bundle over a Riemannian manifold with the help of the parallel transport map associated to some class of covariant derivatives. Through the dual formulations of the proposed models, we obtain the expressions of their solutions, which exhibit the functional spaces that describe the image features. Finally, for a well-chosen covariant derivative and its nonlocal extension, the proposed models perform local contrast modification (reduction or enhancement) and experiments show that they preserve more the aspect of the original image than the Euclidean models do while modifying equally its contrast.

AMS 2000 subject classifications: Primary 49M29, 53C05, 68U10; secondary 90C25, 90C26.

Keywords and phrases: nonlocal variational model, vector bundle, covariant derivative, image contrast reduction/enhancement, primal-dual algorithm.

Contents

| | | |
|-------|--|----|
| 1 | Introduction | 2 |
| 1.1 | Variational techniques for image features regularization and enhancement | 2 |
| 1.2 | Previous work and contribution | 3 |
| 2 | Nonlocal total variation on a vector bundle | 4 |
| 2.1 | Nonlocal vectorial total variation on an Euclidean space | 4 |
| 2.2 | Nonlocal covariant derivative | 6 |
| 2.3 | Nonlocal total variation on a vector bundle | 8 |
| 3 | Variational models for image processing tasks | 12 |
| 3.1 | Image features regularization | 12 |
| 3.1.1 | Previous work | 12 |
| 3.1.2 | The proposed model and its solutions | 13 |
| 3.1.3 | Algorithm to solving the proposed model | 14 |

*This work was supported by the European Research Council, Starting Grant ref. 306337, by the Spanish government, grant ref. TIN2012-38112, and by the Icrea Academia Award.

| | | |
|-------|---|----|
| 3.2 | Image features enhancement | 15 |
| 3.2.1 | Previous work | 15 |
| 3.2.2 | The proposed model and its solutions | 16 |
| 3.2.3 | Algorithm to solving the proposed model | 18 |
| 4 | Applications to local contrast modification | 19 |
| 4.1 | The chosen nonlocal covariant derivative and its numerical implementation | 19 |
| 4.1.1 | The chosen local covariant derivative | 19 |
| 4.1.2 | Nonlocal extension of the chosen covariant derivative | 20 |
| 4.2 | Local contrast reduction | 22 |
| 4.3 | Local contrast enhancement | 23 |
| 4.4 | Functional spaces modeling noise, textures and contrast on color images | 27 |
| 5 | Conclusion and further work | 32 |
| | References | 32 |
| | Author's addresses | 36 |

1. Introduction

1.1. Variational techniques for image features regularization and enhancement

Regularizing or enhancing image features, e.g. noise, textures, edges, contrast, are very useful tasks for correcting defects produced during the acquisition process of a real-world scene and its reproduction on a display, due to physical and technological limitations (see e.g. [6] for more details). These tasks are also useful as pre-processing stage in order to improve the results of higher level applications like pattern recognition. Variational methods are then a very powerful tool for performing regularization or enhancement of image features, and have been extensively used over the last two decades.

Regarding enhancement tasks, a seminal variational approach is due to Sapiro and Caselles [29] for contrast enhancement purpose. Later on, Bertalmío et al. [7] adapted that model to deal with local contrast, and several applications have then been derived from that variational model: perceptual color correction [7],[25], tone mapping [15], color gamut expansion [35], and dehazing [18] to name a few. Connections have also been made between the variational formulation [7] and Retinex theory [8],[9]. As enhancing some features can also yield noise amplification, some techniques combine features enhancement with noise removal (see e.g. [34] for coherence enhancement on color images, [17] for edge enhancement on gray-level images, [2] for color enhancement). Note that these three methods are based on generalized heat diffusions, and do not necessarily arise from a variational formulation. More recently, Fitschen et al. [16] proposed a variational model for contrast enhancement on color images with the total variation (TV) as regularizing term.

The Rudin-Osher-Fatemi (ROF) denoising model [28] based on minimizing

the TV of the image has been a pioneering approach for removing noise from images. However, as it has also a tendency to smooth textures and reduce the contrast of the image, several modifications of the TV have then been proposed in order to tackle those issues (see e.g. [10],[36] for second order derivatives-based regularizers and [4],[11],[20] for vectorial extensions of the TV). On the other hand, since the seminal nonlocal approaches of Buades et al. [12] and Awate et al. [1] for image denoising, several nonlocal variational formulations for image regularization have been proposed (see e.g. [19],[21],[22]). In particular, Gilboa and Osher [19] introduced the concept of nonlocal gradient operator from which they derive a nonlocal total variation (TV_w^{NL}), associated to some weight function w . Whereas the aforementioned models in this paragraph are devoted to noise or irregularities removal, the contrast enhancement model of Bertalmío et al. [7] can be slightly modified to produce contrast reduction [8], which has been used by Zamir et al. [35] for color gamut reduction.

1.2. Previous work and contribution

In [4], we extended the ROF denoising model (based on TV) and its vectorial extension proposed by Bresson and Chan [11] (based on a vectorial extension of TV, called VTV) to a vector bundle over a Riemannian manifold, replacing the Euclidean gradient operator in the expression of TV and the Jacobian operator in the expression of VTV by a covariant derivative. In particular, we showed that, if the covariant derivative is compatible with the vector bundle metric, then the corresponding total variation VBTv possesses a dual formulation from which follows an expression of the unique solution of the variational model. We also derived from the dual formulation of the variational problem an algorithm to compute the numerical solution, based on Chambolle’s projection algorithm [13]. For a well-chosen covariant derivative, we showed that our model preserves better the edges and textures of the original image than the TV-based model for gray-level images and the VTV-based model for color images. Moreover, it also outperforms these “Euclidean” models in terms of objective measures, namely the Peak Signal-to-Noise Ratio (PSNR) and the image Quality index (Q-index) [32], this latter being more correlated to perception than the PSNR [26].

Based on the observation that the nonlocal regularization model of Gilboa and Osher [19] associated to the so-called anisotropic TV_w^{NL} and the contrast enhancement model of Bertalmío et al. [7] are similar up to the sign of the anisotropic TV_w^{NL} in their variational formulations, we established in [5] some connections between the solutions of these models. Under their dual formulations, we showed that the expressions of the solutions both exhibit the same functional space, which is a nonlocal extension of the space of oscillating patterns [24] that is involved in the expression of the solution of the ROF model. We then showed that Chambolle’s projection algorithm can be extended to the nonlocal case to solve the (convex) regularization model and can be adapted to deal with the (non convex) enhancement model and approximate a solution. Note that we showed that these results also hold in the vectorial setting, i.e.

when considering a nonlocal vectorial total variation VTV_w^{NL} .

This paper can be viewed as an unification of our two previous works aforementioned: we extend the nonlocal models studied in [5] from the Euclidean space to a vector bundle over a Riemannian manifold equipped with a vector bundle metric, as we did in the local case in [4]. For this, we introduce the concept of nonlocal covariant derivative on a vector bundle, by the use of the parallel transport map associated to a covariant derivative. We then construct a nonlocal total variation $\text{VBTV}_w^{\text{NL}}$ induced by the nonlocal covariant derivative and we show that it possesses a dual formulation provided that the (local) covariant derivative is compatible with the vector bundle metric. By the use of the dual formulations of the corresponding variational models, we obtain expressions of their solutions, and we show that they can be computed numerically through primal-dual algorithms (see e.g. [14]), which are known to be more efficient than the projection algorithm we were using in [5]. The expressions of the solutions also exhibit a class of functional spaces, which can be viewed as nonlocal and non Euclidean extensions of the space of oscillating patterns aforementioned. Finally, taking the covariant derivative compatible with the vector bundle metric constructed in [3] and w as a Gaussian kernel, experiments show that these functional spaces can model noise, textures and contrast on color images, and the variational models perform local contrast modification (reduction or enhancement) that preserves more the aspect of the original image than their ‘‘Euclidean’’ restrictions in [5] while modifying equally its contrast.

2. Nonlocal total variation on a vector bundle

2.1. Nonlocal vectorial total variation on an Euclidean space

The aim of this section is to remind the reader of the definition of vectorial nonlocal total variation VTV_w^{NL} we introduced in [5].

Definition 2.1 (Nonlocal gradient operator). *Let Ω be a compact subset of \mathbb{R}^2 and $u: \Omega \rightarrow \mathbb{R}^n$ be a smooth vector-valued function. We assume that \mathbb{R}^n is equipped with a positive definite quadratic form h . A nonlocal gradient is an operator $\nabla_w^{\text{NL}}: C^\infty(\Omega; \mathbb{R}^n) \rightarrow C^\infty(\Omega \times \Omega; \mathbb{R}^n)$ of the form*

$$\nabla_w^{\text{NL}} u: (x, y) \mapsto w(x, y) (u(y) - u(x)) \quad (1)$$

and $w: \Omega \times \Omega \rightarrow \mathbb{R}^{+*}$ is a smooth symmetric function.

Note that formula (1) is nothing but the vectorial extension of the nonlocal gradient introduced by Gilboa and Osher [19] for real-valued functions.

Standard choices for the weight function w in the context of image processing are Euclidean/Riemannian distance, Gaussian kernel, and patch-based distances. We refer to Zosso et al. [33] for more details as well as for the definition of a weight function specific to color images determined by the hue difference between two colors. The choice of the positive definite quadratic form h greatly

depends on the nature of the image to be processed. Dealing with color images, a suitable choice for h is the perceptual metric associated to the color space involved (e.g. the Euclidean metric associated to the CIE Lab color space).

Definition 2.2 (The space $W_{w,1,p}^{NL}(\Omega; \mathbb{R}^n)$). *The quadratic form h induces a scalar product $\langle \cdot, \cdot \rangle$ on $C^\infty(\Omega \times \Omega; \mathbb{R}^n)$ defined by*

$$\langle \eta_1, \eta_2 \rangle := \int_{\Omega \times \Omega} (\eta_1(x, y), \eta_2(x, y))_h dx dy,$$

where $(\cdot, \cdot)_h$ denotes the scalar product with respect to h . The L^p norm on $C^\infty(\Omega \times \Omega; \mathbb{R}^n)$ is defined by

$$\|\eta\|_{L^p} := \left(\int_{\Omega \times \Omega} \|\eta(x, y)\|_h^p dx dy \right)^{1/p}$$

where $\|\cdot\|_h$ denotes the norm associated to h . In particular, we have

$$\|\nabla_w^{NL} u\|_{L^p} = \left(\int_{\Omega \times \Omega} \|w(x, y)(u(y) - u(x))\|_h^p dx dy \right)^{1/p}. \quad (2)$$

Finally, we define the space

$$W_{w,1,p}^{NL}(\Omega; \mathbb{R}^n) := \{u \in L^p(\Omega; \mathbb{R}^n) : \nabla_w^{NL} u \in L^p(\Omega \times \Omega; \mathbb{R}^n)\}.$$

Assuming that the function u is real-valued, the norm $\|\nabla_w^{NL} u\|_{L^1}$ corresponds to the anisotropic TV_w^{NL} introduced by Gilboa and Osher [19], as well as the contrast modification term in the perceptual color correction model proposed by Bertalmío et al. [7].

Definition 2.3 (Adjoint of a nonlocal gradient operator). *We define the adjoint of the operator ∇_w^{NL} as the operator $\nabla_w^{NL*} : C^\infty(\Omega \times \Omega; \mathbb{R}^n) \rightarrow C^\infty(\Omega; \mathbb{R}^n)$ satisfying*

$$\langle \nabla_w^{NL} u, \eta \rangle = (u, \nabla_w^{NL*} \eta)$$

$\forall u \in C^\infty(\Omega; \mathbb{R}^n), \forall \eta \in C^\infty(\Omega \times \Omega; \mathbb{R}^n)$, where (\cdot, \cdot) is the L^2 scalar product on $C^\infty(\Omega; \mathbb{R}^n)$ induced by h .

As in the scalar case in [19], a straightforward computation yields

$$\nabla_w^{NL*} \eta : x \mapsto \int_{\Omega} w(x, y)(\eta(y, x) - \eta(x, y)) dy. \quad (3)$$

We derive from Def. 2.3 the definition of VTV_w^{NL} on the set $L^1(\Omega; \mathbb{R}^n)$.

Definition 2.4 (Nonlocal vectorial total variation). *The nonlocal vectorial total variation $\text{VTV}_w^{NL}(u)$ of $u \in L^1(\Omega; \mathbb{R}^n)$ is the quantity*

$$\sup_{\eta \in \mathcal{H}_1} \left(\int_{\Omega} (u, \nabla_w^{NL*} \eta)_h d\Omega \right) \quad (4)$$

where the set \mathcal{H}_a , for $a \in \mathbb{R}^{+*}$, is

$$\mathcal{H}_a := \{\eta \in C^\infty(\Omega \times \Omega; \mathbb{R}^n), \|\eta(x, y)\|_h \leq a \ \forall x, y \in \Omega\}. \quad (5)$$

Note that we can also write

$$VTV_w^{NL}(u) = \sup_{\xi \in K_1} \left(\int_{\Omega} (u, \xi)_h \, d\Omega \right), \quad (6)$$

where the set K_a is the closure in $L^2(\Omega; \mathbb{R}^n)$ of the set \mathcal{K}_a defined by

$$\mathcal{K}_a := \left\{ \nabla_w^{NL*} \eta : \eta \in C^\infty(\Omega \times \Omega; \mathbb{R}^n), \|\eta(x, y)\|_h \leq a \ \forall x, y \in \Omega \right\}. \quad (7)$$

We denote by $BV_w^{NL}(\Omega; \mathbb{R}^n)$ the set of functions $u \in L^1(\Omega; \mathbb{R}^n)$ such that $VTV_w^{NL}(u) < +\infty$.

Proposition 2.1. *If $u \in W_{w,1,1}^{NL}(\Omega; \mathbb{R}^n)$ then,*

$$VTV_w^{NL}(u) = \|\nabla_w^{NL} u\|_{L^1}. \quad (8)$$

Proof. Prop.2.1 is a particular case of Prop.2.3 whose proof is detailed below. \square

2.2. Nonlocal covariant derivative

In order to extend VTV_w^{NL} from the Euclidean space to a vector bundle over a Riemannian manifold, we need first to extend the concept of nonlocal gradient operator to a vector bundle. Our proposal is then to make use of the parallel transport map associated to a covariant derivative. We first remind the definitions of these two objects.

Let E be a vector bundle over a complete Riemannian manifold (M, g) and $\pi: E \rightarrow M$ the projection map. In this paper, we denote by E_x the fiber over $x \in M$, i.e. the set $\{\pi^{-1}(x)\}$, and by $\Gamma(E)$ the set of smooth sections of E . We denote by TM resp. T^*M the tangent bundle resp. the cotangent bundle of M , and by $\bigwedge^k T^*M$ the vector bundle of differential k -forms of M . We denote by $\text{End}(E)$ the bundle of fiber-wise endomorphisms of E . Finally, we denote by $pr_1(E)$ the vector bundle over $M \times M$ induced by the projection

$$\begin{aligned} M \times M &\longrightarrow M \\ pr_1 : (x, y) &\longmapsto x \end{aligned}$$

In others words

$$pr_1(E) = \{(x, y, p) \in M \times M \times E / x = \pi(p)\} \quad (9)$$

Definition 2.5 (Covariant derivative). *A covariant derivative (or connection) on E is a map $\nabla: \Gamma(TM) \times \Gamma(E) \rightarrow \Gamma(E)$ of the form*

$$\nabla_X \varphi = d_X \varphi + \omega(X)\varphi \quad (10)$$

where $X \in \Gamma(TM)$, d stands for the differential operator acting on the components of the sections and $\omega \in \Gamma(T^*M \otimes \text{End}(E))$ is called a **connection 1-form**.

Hence, a covariant derivative is completely determined by a connection 1-form. The covariant derivative induced by the connection 1-form $\omega \equiv 0$ is called **trivial covariant derivative**.

Definition 2.6 (Parallel transport). *Let $\gamma: I \subset \mathbb{R} \rightarrow M$ be a smooth curve. The parallel transport associated to a covariant derivative ∇ on E along the curve γ is the map $\tau_{\gamma, t_1, t_2}: E_{\gamma(t_1)} \rightarrow E_{\gamma(t_2)}$ such that $\tau_{\gamma, t_1, t_2}(\varphi_0)$ is the solution of the differential equation*

$$\begin{cases} \nabla_{\gamma'(t)} \varphi \circ \gamma(t) = 0 & \forall t \in [t_1, t_2] \\ \varphi \circ \gamma(t_1) = \varphi_0 \end{cases} \quad (11)$$

We have now available the tools to introduce the concept of nonlocal covariant derivative on a vector bundle. We distinguish two cases, whether the covariant derivative is flat or not.

Definition 2.7 (Flat covariant derivative). *The curvature associated to a covariant derivative ∇ is the tensor $R \in \Gamma(\wedge^2 T^*M \otimes \text{End } E)$ defined by*

$$R(X, Y)\varphi = \nabla_X \nabla_Y \varphi - \nabla_Y \nabla_X \varphi - \nabla_{[X, Y]}\varphi \quad (12)$$

where $X, Y \in \Gamma(TM)$ and $\varphi \in \Gamma(E)$.

The covariant derivative ∇ is said **flat** if its curvature tensor vanishes identically.

Then, based on the fact that the parallel transport associated to a flat covariant derivative between two points is independent of the curve joining these two points, we propose the following definition.

Definition 2.8 (nonlocal covariant derivative: the case of flat covariant derivative). *The nonlocal covariant derivative associated to a flat covariant derivative ∇ is an operator $\nabla_w^{NL}: \Gamma(E) \rightarrow \Gamma(\text{pr}_1(E))$ of the form*

$$\nabla_w^{NL} \varphi: (x, y) \mapsto w(x, y) \left(\tau_{\gamma(x, y), 0, l(\gamma(x, y))}^{-1} \varphi(y) - \varphi(x) \right) \quad (13)$$

for any smooth curve $\gamma_{(x, y)}$ starting at x and ending at y , where $l(\gamma_{(x, y)})$ denotes its length, and where w is a symmetric positive function.

As the map $\tau_{\gamma(x, y), 0, l(\gamma(x, y))}^{-1}$ only depends on x and y , we rewrite (13) as

$$\nabla_w^{NL} \varphi: (x, y) \mapsto w(x, y) \left(\tau_{x, y}^{-1} \varphi(y) - \varphi(x) \right) \quad (14)$$

We can then observe that formulae (13) and (14) restrict to the “Euclidean” nonlocal gradient operator (1) when ∇ is taken as the trivial covariant derivative.

In order to adapt formula (13) to non flat covariant derivatives, we need to specify the curves along which we perform the parallel transport. A natural choice is then to consider the geodesics of (M, g) , and this yields the following definition.

Definition 2.9 (nonlocal covariant derivative: general case). *The nonlocal covariant derivative associated to a covariant derivative ∇ is an operator $\nabla_w^{NL} : \Gamma(E) \rightarrow \Gamma(\text{pr}_1(E))$ of the form*

$$\nabla_w^{NL} \varphi : (x, y) \mapsto w(x, y) \left(\frac{1}{\#\{\gamma_{(x,y)}^{min}\}} \sum_{\{\gamma_{(x,y)}^{min}\}} \tau_{\gamma_{(x,y)}^{min}, 0, d_g(x,y)}^{-1} \varphi(y) - \varphi(x) \right) \quad (15)$$

where $\{\gamma_{(x,y)}^{min}\}$ is the set of geodesics starting at x and ending at y parametrized by the arc length, $d_g(x, y)$ the geodesic distance between x and y , i.e. the length of the curves $\gamma_{(x,y)}^{min}$, and where w is a symmetric positive function.

Both definitions are indeed compatible since formula (15) does reduce to (13) if ∇ is flat.

2.3. Nonlocal total variation on a vector bundle

In this section, we introduce the concept of nonlocal total variation VBTV_w^{NL} for integrable sections of a vector bundle equipped with a definite positive metric and a covariant derivative compatible with that metric. We first remind the reader of some definitions and results related to covariant derivatives compatible with a vector bundle metric.

Definition 2.10. *A metric h on a vector bundle E over a manifold M is the assignment of a scalar product h_x on each fiber $\{\pi^{-1}(x)\}$, $x \in M$. The metric is said positive definite if the scalar products are positive definite.*

Definition 2.11. *A covariant derivative ∇ is compatible with the vector bundle metric h if it satisfies*

$$dh(\varphi, \psi) = (\nabla\varphi, \psi)_h + (\varphi, \nabla\psi)_h \quad (16)$$

for any $\varphi, \psi \in \Gamma(E)$.

It follows from Def. 2.11 that the parallel transport $\tau_{\gamma,t,s}$ along any smooth curve γ associated to a covariant derivative compatible with a metric h is an isometry $(E_{\gamma(t)}, h_{\gamma(t)}) \rightarrow (E_{\gamma(s)}, h_{\gamma(s)})$.

Moreover, there is a one-one correspondence between connection 1-forms ω that are $\mathfrak{so}(h)$ -valued i.e. $\omega \in \Gamma(T^*M \otimes \mathfrak{so}(h))$ and covariant derivatives ∇ that

are compatible with the metric h . We refer to Lawson and Michelson ([23], Prop. 4.4 p.103) for a proof of that result.

From now on, we assume that E is equipped with a positive definite metric h , and ∇ is a connection compatible with h . Under this latter assumption, the nonlocal covariant derivative (15) possesses an adjoint operator, that we will define below. We first introduce a norm on the space $\Gamma(pr_1(E))$, defined in formula (9).

The positive definite metric h on E induces a L^2 scalar product $\langle \cdot, \cdot \rangle$ on $\Gamma(pr_1(E))$ defined by

$$\langle \eta_1, \eta_2 \rangle := \int_{M \times M} (\eta_1(x, y), \eta_2(x, y))_{h_x} dx dy$$

where $(\cdot, \cdot)_{h_x}$ denotes the scalar product in E_x with respect to $h(x)$, from which derive the L^p norm on $\Gamma(pr_1(E))$ defined by

$$\|\eta\|_{L^p} := \left(\int_{M \times M} \|\eta(x, y)\|_{h_x}^p dx dy \right)^{1/p}$$

where $\|\cdot\|_{h_x}$ denotes the norm associated to $h(x)$, and the space $L^p(pr_1(E))$ as the completion of $\Gamma(pr_1(E))$ in this norm.

Finally, we define the space

$$W_{w,1,p}^{NL} := \{\varphi \in L^p(E), \nabla_w^{NL} \varphi \in L^p(pr_1(E))\}$$

Definition 2.12 (Adjoint of nonlocal covariant derivative). *The adjoint of a nonlocal covariant derivative ∇_w^{NL} induced by a covariant derivative ∇ compatible with a positive definite metric h is the operator $\nabla_w^{NL*} : \Gamma(pr_1(E)) \rightarrow \Gamma(E)$ satisfying*

$$\langle \nabla_w^{NL} \varphi, \eta \rangle = \langle \varphi, \nabla_w^{NL*} \eta \rangle$$

$\forall \varphi \in \Gamma(E), \forall \eta \in \Gamma(pr_1(E))$, where (\cdot, \cdot) is the L^2 scalar product on $\Gamma(E)$ induced by h .

Proposition 2.2. *The operator ∇_w^{NL*} is defined by*

$$\nabla_w^{NL*} \eta : x \rightarrow \int_M w(x, y) \left(\frac{1}{\#\{\gamma_{(x,y)}^{min}\}} \sum_{\{\gamma_{(x,y)}^{min}\}} \tau_{\gamma_{(x,y)}^{min}, 0, d_g(x,y)}^{-1} \eta(y, x) - \eta(x, y) \right) dy \quad (17)$$

Proof. We have

$$\begin{aligned} \langle \nabla_w^{NL} \varphi, \eta \rangle &= \int_{M \times M} w(x, y) \left[\frac{1}{\#\{\gamma_{(x,y)}^{min}\}} \sum_{\{\gamma_{(x,y)}^{min}\}} \left((\tau_{\gamma_{(x,y)}^{min}, 0, d_g(x,y)}^{-1} \varphi(y) - \varphi(x)), \eta(x, y) \right)_{h_x} \right] dx dy \\ &= \int_{M \times M} w(x, y) \left[\frac{1}{\#\{\gamma_{(x,y)}^{min}\}} \sum_{\{\gamma_{(x,y)}^{min}\}} \left((\varphi(y), \tau_{\gamma_{(x,y)}^{min}, 0, d_g(x,y)} \eta(x, y))_{h_y} - (\varphi(x), \eta(x, y))_{h_x} \right) \right] dx dy \end{aligned}$$

since $\tau_{\gamma_{(x,y)}^{min}, 0, d_g(x,y)}: (E_x, h_x) \longrightarrow (E_y, h_y)$ is an isometry, by compatibility of ∇ with h .

It then follows

$$= \int_{M \times M} w(x, y) \left[\frac{1}{\#\{\gamma_{(x,y)}^{min}\}} \sum_{\{\gamma_{(y,x)}^{min}\}} \left((\varphi(x), \tau_{\gamma_{(y,x)}^{min}, 0, d_g(x,y)} \eta(y, x))_{h_x} - (\varphi(x), \eta(x, y))_{h_x} \right) \right] dx dy$$

by interchanging x and y in the first part of the integral, and using the symmetry of w and d_g .

Rearranging the terms and using $\tau_{\gamma_{(y,x)}^{min}, 0, d_g(x,y)} = \tau_{\gamma_{(x,y)}^{min}, 0, d_g(x,y)}^{-1}$, we finally obtain

$$\langle \nabla_w^{NL} \varphi, \eta \rangle = \int_{M \times M} \left(\varphi(x), w(x, y) \left[\frac{1}{\#\{\gamma_{(x,y)}^{min}\}} \sum_{\{\gamma_{(x,y)}^{min}\}} \tau_{\gamma_{(x,y)}^{min}, 0, d_g(x,y)}^{-1} \eta(y, x) - \eta(x, y) \right] \right)_{h_x} dx dy$$

from which we deduce (17). \square

Definition 2.13 (Nonlocal vectorial total variation of integrable sections). *Let $\varphi \in L^1(E)$ and $w: M \times M \longrightarrow \mathbb{R}^{+*}$ be a smooth symmetric function, we define the **nonlocal vectorial total variation** $VBTV_w^{NL}(\varphi)$ of φ as the quantity*

$$\sup_{\eta \in \mathcal{H}_1} \left(\int_M (\varphi, \nabla_w^{NL*} \eta)_h dM \right) \quad (18)$$

where the set \mathcal{H}_a , for $a \in \mathbb{R}^{+*}$, is

$$\mathcal{H}_a := \{ \eta \in \Gamma(pr_1(E)), \|\eta(x, y)\|_{h_x} \leq a \ \forall x, y \in M \} \quad (19)$$

We can also write

$$VBTV_w^{NL}(\varphi) = \sup_{\xi \in K_1} \left(\int_M (\varphi, \xi)_h dM \right) \quad (20)$$

where K_a is the closure in $L^2(E)$ of the set \mathcal{K}_a defined by

$$\mathcal{K}_a := \{ \nabla_w^{NL*} \eta : \eta \in \Gamma(pr_1(E)), \|\eta(x, y)\|_{h_x} \leq a \ \forall x, y \in M \} \quad (21)$$

We denote by $BV_w^{NL}(E)$ the set of sections $\varphi \in L^1(E)$ such that $VBTV_w^{NL}(\varphi) < +\infty$.

Proposition 2.3. *If $\varphi \in W_{w,1,1}^{NL}(E)$ then,*

$$VBTV_w^{NL}(\varphi) = \|\nabla_w^{NL} \varphi\|_{L^1} \quad (22)$$

Proof. Let $\eta \in \Gamma(pr_1(E))$, we have

$$\int_M (\varphi, \nabla_w^{NL*} \eta)_h dM = \int_{M \times M} \langle \nabla_w^{NL} \varphi, \eta \rangle_h dM \times M$$

by definition of the adjoint operator ∇_w^{NL*} .

Then, as the metric h is positive definite, we have

$$\int_{M \times M} \langle \nabla_w^{NL} \varphi, \eta \rangle_h dM \times M \leq \int_{M \times M} \|\nabla_w^{NL} \varphi\|_h \|\eta\|_h dM \times M$$

and it follows

$$\int_{M \times M} \|\nabla_w^{NL} \varphi\|_h \|\eta\|_h dM \times M \leq \int_{M \times M} \|\nabla_w^{NL} \varphi\|_h dM \times M$$

since $\|\eta(x, y)\|_{h_x} \leq 1 \quad \forall (x, y) \in M \times M$. Hence

$$\sup_{\eta \in \mathcal{H}_1} \left(\int_M (\varphi, \nabla_w^{NL*} \eta)_h dM \right) \leq \int_{M \times M} \|\nabla_w^{NL} \varphi\|_h dM \times M \quad (23)$$

Let

$$\tilde{\eta}: (x, y) \mapsto \begin{cases} \frac{\nabla_w^{NL} \varphi(x, y)}{\|\nabla_w^{NL} \varphi(x, y)\|_{h_x}} & \text{if } \nabla_w^{NL} \varphi(x, y) \neq 0 \\ 0 & \text{otherwise} \end{cases} \quad (24)$$

and $(\eta_\epsilon) \in \Gamma(pr_1(E))$, $\|\eta_\epsilon(x, y)\|_{h_x} \leq 1 \quad \forall (x, y) \in M \times M$ such that $\eta_\epsilon \xrightarrow{\epsilon \rightarrow 0} \tilde{\eta}$. We claim that such a sequence can be constructed using generalizations of Lusin's theorem and the mollification technique to vector-valued measurable functions.

We then have

$$\begin{aligned} \lim_{\epsilon \rightarrow 0} \int_M (\varphi, \nabla_w^{NL*} \eta_\epsilon)_h dM &= \lim_{\epsilon \rightarrow 0} \int_{M \times M} \langle \nabla_w^{NL} \varphi, \eta_\epsilon \rangle_h dM \times M \\ &= \int_{M \times M} \langle \nabla_w^{NL} \varphi, \tilde{\eta} \rangle_h dM \times M \\ &= \int_{\{\nabla_w^{NL} \varphi \neq 0\}} \left\langle \nabla_w^{NL} \varphi, \frac{\nabla_w^{NL} \varphi}{\|\nabla_w^{NL} \varphi\|_h} \right\rangle_h dM \times M \\ &= \int_{M \times M} \|\nabla_w^{NL} \varphi\|_h dM \times M \end{aligned}$$

Hence, we have constructed a sequence $\int_M (\varphi, \nabla_w^{NL*} \eta_\epsilon)_h dM$ converging towards $\int_{M \times M} \|\nabla_w^{NL} \varphi\|_h dM \times M$, and such that

$$\int_M (\varphi, \nabla_w^{NL*} \eta_\epsilon)_h dM \leq \int_{M \times M} \|\nabla_w^{NL} \varphi\|_h dM \times M \quad \forall \epsilon$$

since $\|\eta_\epsilon(x, y)\|_{h_x} \leq 1 \quad \forall (x, y) \in M \times M$. Together with (23), it shows that

$$\sup_{\eta \in \mathcal{H}_1} \left(\int_M (\varphi, \nabla_w^{NL*} \eta)_h dM \right) = \int_{M \times M} \|\nabla_w^{NL} \varphi\|_h dM \times M$$

□

In what follows, we highlight two properties of VBTV_w^{NL} that will be useful in the next Section where we consider variational models based on VBTV_w^{NL} .

Properties of VBTV_w^{NL} :

Let us first notice that VBTV_w^{NL} is a sup of linear forms

$$J_\eta: \varphi \mapsto \int_M (\varphi, \nabla_w^{NL*} \eta)_h dM \quad \text{s.t. } \eta \in \mathcal{H}_1$$

which are continuous with respect to the weak topology of $L^2(E)$ since they are bounded. Hence, for $\varphi \in L^2(E)$ and $\varphi_n \rightharpoonup \varphi$, we have $J_\eta(\varphi_n) \rightarrow J_\eta(\varphi)$.

1. Lower semi-continuity

We have

$$J_\eta(\varphi) = \lim_n J_\eta(\varphi_n) \leq \liminf_n \text{VBTV}_w^{NL}(\varphi_n)$$

and taking the sup over the set \mathcal{H}_1 yields

$$\text{VBTV}_w^{NL}(\varphi) \leq \liminf_n \text{VBTV}_w^{NL}(\varphi_n)$$

meaning that VBTV_w^{NL} is lower semi-continuous with respect to the weak topology of $L^2(E)$.

2. Convexity The functional VBTV_w^{NL} is convex as the supremum of the convex (since linear) functionals J_η . Indeed, $\forall \varphi_1, \varphi_2 \in L^1(E)$, we have

$$\begin{aligned} J_\eta(t\varphi_1 + (1-t)\varphi_2) &= tJ_\eta(\varphi_1) + (1-t)J_\eta(\varphi_2) \\ &\leq t\text{VBTV}_w^{NL}(\varphi_1) + (1-t)\text{VBTV}_w^{NL}(\varphi_2) \end{aligned}$$

and consequently

$$\text{VBTV}_w^{NL}(t\varphi_1 + (1-t)\varphi_2) \leq t\text{VBTV}_w^{NL}(\varphi_1) + (1-t)\text{VBTV}_w^{NL}(\varphi_2)$$

3. Variational models for image processing tasks

3.1. Image features regularization

3.1.1. Previous work

In [19], Gilboa and Osher developed a nonlocal variational formulation based on the so-called anisotropic nonlocal total variation for the regularization of

gray-level images $u_0: \Omega \subset \mathbb{R}^2 \rightarrow \mathbb{R}$, that can be written as follows with our notations

$$\arg \min_u \frac{\lambda}{2} \|u - u_0\|_{L^2}^2 + \|\nabla_w^{NL} u\|_{L^1} \quad (25)$$

for $\lambda > 0$, where $\|\nabla_w^{NL} u\|_{L^1}$ is of the form (2) for $n = 1$.

In [5], we showed that we can derive an expression of the unique solution of the problem (25), and of its vectorial extension, using the dual formulation VTV_w^{NL} of the term $\|\nabla_w^{NL}\|_{L^1}$, defined in (4).

More precisely, we considered the following variational problem

$$\arg \min_{u \in L^2 \cap BV_w^{NL}(\Omega; \mathbb{R}^n)} \frac{\lambda}{2} \|u - u_0\|_{L^2}^2 + VTV_w^{NL}(u) \quad (26)$$

and showed that its unique solution \underline{u} is of the form

$$\underline{u} = u_0 - P_{K_{1/\lambda}} u_0 \quad (27)$$

where P is the projection operator, and $K_{1/\lambda}$ is the closure in $L^2(\Omega; \mathbb{R}^n)$ of the set $\mathcal{K}_{1/\lambda}$ defined in (7).

3.1.2. The proposed model and its solutions

Let us first point out that the variational problem (26) can be rewritten in the vector bundle context proposed in this paper when viewing a \mathbb{R}^n -valued function on Ω as a section of a (trivial) vector bundle over Ω , and considering the regularizing term VTV_w^{NL} in (26) as the (vector bundle) nonlocal total variation $VBTV_w^{NL}$ (18) induced by the trivial covariant derivative and the vector bundle metric consisting in the Euclidean scalar product in each fiber.

The following proposition shows that the problem (26) extends in a straightforward way when replacing the trivial covariant derivative by a non trivial one, assuming that this latter is compatible with a vector bundle positive definite metric.

Proposition 3.1. *Let E be a vector bundle over a complete Riemannian manifold (M, g) equipped with a positive definite metric h and a covariant derivative ∇ compatible with h , and $u_0 \in L^2(E)$. The unique solution \underline{u} of the variational problem*

$$\arg \min_{u \in L^2 \cap BV_w^{NL}(E)} \frac{\lambda}{2} \|u - u_0\|_{L^2}^2 + VBTV_w^{NL}(u) \quad (28)$$

is

$$\underline{u} = u_0 - P_{K_{1/\lambda}} u_0 \quad (29)$$

where P is the projection operator, and $K_{1/\lambda}$ is the closure in $L^2(E)$ of the set $\mathcal{K}_{1/\lambda}$ defined in (21).

Proof. As proved in Sect. 2, the functional $VBTV_w^{NL}$ is lower semicontinuous convex, and is also proper. Hence, the regularization model (28) is the proximity operator of $\frac{1}{\lambda}VBTV_w^{NL}$ evaluated at the element u_0 . Then, according to Moreau's decomposition formula (see. e.g. [27] for details), we have

$$\underline{u} = u_0 - \frac{1}{\lambda} \operatorname{prox}(\lambda VBTV_w^{NL*})(\lambda u_0) \quad (30)$$

By definition, $VBTV_w^{NL}$ is the support function of the closure K_1 of the convex set \mathcal{K}_1 . Hence its convex conjugate $VBTV_w^{NL*}$ is the indicator function δ_{K_1} of K_1 . We then have

$$\begin{aligned} \operatorname{prox}(\lambda VBTV_w^{NL*})(\lambda u_0) &:= \arg \min_v \frac{1}{2\lambda} \|v - \lambda u_0\|_{L^2(E)}^2 + \delta_{K_1}(v) \\ &= \arg \min_{v \in K_1} \|v/\lambda - u_0\|_{L^2(E)}^2 \\ &= \lambda \arg \min_{v \in K_{1/\lambda}} \|v - u_0\|_{L^2(E)}^2 \\ &= \lambda P_{K_{1/\lambda}} u_0 \end{aligned}$$

Together with (30), it follows formula (29). \square

3.1.3. Algorithm to solving the proposed model

The original problem (28) has the following primal-dual formulation

$$\min_{u \in L^2(E)} \max_{\eta \in \mathcal{H}_1} \mathcal{L}(u, \eta) := \frac{\lambda}{2} \|u - u_0\|_{L^2}^2 + (u, \nabla_w^{NL*} \eta) \quad (31)$$

The function \mathcal{L} is strictly convex in u and concave in η , which guarantees that the saddle points of \mathcal{L} are of the form (\underline{u}, η) , where \underline{u} is the unique solution of the primal problem (28) and η is a solution of its dual formulation. In the discrete setting, the problem (31) can be rewritten

$$\min_{u \in L^2(E)} \max_{\eta \in \mathcal{H}_1} \frac{\lambda}{2} \|u - u_0\|_{L^2}^2 + \langle \nabla_w^{NL} u, \eta \rangle,$$

which is equivalent to

$$\min_{u \in L^2(E)} \max_{\eta \in \Gamma(pr_1(E))} \langle \nabla_w^{NL} u, \eta \rangle + \frac{\lambda}{2} \|u - u_0\|_{L^2}^2 - \delta_{\mathcal{H}_1}(\eta) \quad (32)$$

Problem (32) is of the form

$$\min_{u \in X} \max_{\eta \in Y} \langle Au, v \rangle + G(u) - F^*(v) \quad (33)$$

where X, Y are two finite-dimensional real vector spaces equipped with an inner product, the map $A: X \rightarrow Y$ is a continuous linear operator possessing an

adjoint A^* , the maps $G: X \rightarrow [0, +\infty]$, $F^*: Y \rightarrow [0, +\infty]$ are proper, convex, lower semi-continuous, and F^* is the convex conjugate of a convex lower semi-continuous function F . Then, the solutions of these problems satisfy

$$A\underline{u} \in \partial F^*(\underline{\eta}) \quad (34)$$

$$-A^*\underline{\eta} \in \partial G^*(\underline{u}) \quad (35)$$

where ∂ denotes the sub-differential operator.

The problem (33) can be solved through one of the primal-dual algorithms presented in Chambolle and Pock [14]. Dealing with the Arrow-Hurwicz approach with fixed step sizes, the algorithm to solving (31) reads

- * Initialization: Choose $\tau, \sigma > 0$ s.t. $\tau\sigma\|A\|^2 \leq 1$, $(u^0, \eta^0) \in L^2(E) \times \Gamma(pr_1(E))$.
- * Iterations ($n \geq 0$): Update u^n, η^n as follows:

$$\begin{cases} \eta^{n+1} = (I + \sigma\partial F^*)^{-1}(\eta^n + \sigma A u^n) \\ u^{n+1} = (I + \tau\partial G)^{-1}(u^n - \tau A^* \eta^{n+1}) \end{cases} \quad (36)$$

In the context of problem (31), the iterative procedure is then the following

$$\begin{cases} \eta^{n+1} = \frac{\eta^n + \sigma \nabla_w^{NL} u^n}{\max(1, \|\eta^n + \sigma \nabla_w^{NL} u^n\|_h)} \\ u^{n+1} = \frac{1}{1 + \lambda\tau} [\lambda\tau u_0 + (u_n - \tau \nabla_w^{NL*} \eta^{n+1})] \end{cases} \quad (37)$$

The convergence of the algorithm towards a saddle point is proved in [14].

3.2. Image features enhancement

3.2.1. Previous work

In [7], Bertalmío et al. proposed a variational model for enhancing the local contrast of a color image $u_0 = (u_0^1, u_0^2, u_0^3)$ based on some properties of the human visual system, that can be written as follows with our notations

$$\arg \min_{u^k} \frac{\lambda}{2} \|u^k - u_0^k\|_{L^2}^2 - \|\nabla_w^{NL} u^k\|_{L^1}, \quad k = 1, 2, 3 \quad (38)$$

for $\lambda > 0$, and where $\|\nabla_w^{NL} u\|_{L^1}$ is of the form (2) for $n = 1$.

They showed that the problem (38) has a solution in the discrete case, i.e. when the image domain Ω is considered as discrete. Moreover, in order to approximate a solution, they considered a regularized version of the problem by regularizing the terms $\|\nabla_w^{NL} u^k\|_{L^1}$ and performed a gradient descent until reaching a steady-state.

In [5], we showed that we can derive an expression of the solutions of the original problem (38) and its vectorial extension by the use of the dual formulation $VTV_w^{NL}(u)$ of the term $\|\nabla_w^{NL}u\|_{L^1}$ defined in (4) with $n = 3$, i.e. by considering the model

$$\arg \min_u \frac{\lambda}{2} \|u - u_0\|_{L^2}^2 - VTV_w^{NL}(u) \quad (39)$$

assuming that the solutions belong to the discrete space $L^2 \cap BV_w^{NL}(\Omega; \mathbb{R}^3)$. We then showed that the solutions \underline{u} are of the form

$$\underline{u} = u_0 - \arg \max_{u^* \in \mathcal{K}_{1/\lambda}} \|u_0 - u^*\|_{L^2}^2 \quad (40)$$

and $\mathcal{K}_{1/\lambda}$ is defined in (7).

3.2.2. The proposed model and its solutions

As the variational problem (26), the variational problem (39) can be rewritten in the vector bundle context proposed in this paper when viewing a \mathbb{R}^n -valued function on Ω as a section of a (trivial) vector bundle over Ω , and considering the regularizing term VTV_w^{NL} in (39) as the (vector bundle) nonlocal total variation $VBTV_w^{NL}$ (18) induced by the trivial covariant derivative and the vector bundle metric consisting in the Euclidean scalar product in each fiber.

The following proposition shows that the problem (39) extends in a straightforward way when replacing the trivial covariant derivative by a non trivial one, assuming that this latter is compatible with a vector bundle positive definite metric.

Proposition 3.2. *Let E be a vector bundle over a discrete Riemannian manifold (M, g) , equipped with a positive definite metric h and a covariant derivative ∇ compatible with h , and $u_0 \in L^2(E)$. The solutions \underline{u} of the variational problem*

$$\arg \min_{u \in L^2 \cap BV_w^{NL}(E)} \frac{\lambda}{2} \|u - u_0\|_{L^2}^2 - VBTV_w^{NL}(u) \quad (41)$$

are

$$\underline{u} = u_0 - \arg \max_{u^* \in \mathcal{K}_{1/\lambda}} \|u_0 - u^*\|_{L^2}^2 \quad (42)$$

where $\mathcal{K}_{1/\lambda}$ is defined in (21).

Proof. The problem (41) is of the form

$$\inf_{u \in X} \{G(u) - F(u)\} \quad (43)$$

where F and G are two lower semi-continuous functionals on a reflexive Banach space X such that F is convex and G satisfies $G(u)/\|u\| \rightarrow \infty$ as $\|u\| \rightarrow \infty$. Then according to Theorem 2.7 in [31], if \underline{u}^* is a solution of the dual problem

$$\inf_{u^* \in X^*} \{F^*(u^*) - G^*(u^*)\} \quad (44)$$

where F^* resp. G^* denotes the convex conjugate of F resp. G , then there exists a solution \underline{u} of the primal problem (43), and the solutions of both problems are connected by the formulas

$$F(\underline{u}) + F^*(\underline{u}^*) = \langle \underline{u}, \underline{u}^* \rangle \quad (45)$$

$$G(\underline{u}) + G^*(\underline{u}^*) = \langle \underline{u}, \underline{u}^* \rangle. \quad (46)$$

Hence, the problem (41) can be solved through its dual problem (44).

The convex conjugate of the functional

$$G: u \mapsto \frac{\lambda}{2} \|u - u_0\|_{L^2}^2$$

is

$$G^*: u^* \longrightarrow \frac{1}{2\lambda} (\|u^*\|_{L^2}^2 + 2\langle u^*, \lambda u_0 \rangle_{L^2}) \quad (47)$$

As the manifold M is discrete, the set \mathcal{K}_1 is close and convex, hence the functional $F := VBTV_w^{NL}$ is the support function of \mathcal{K}_1 , and its convex conjugate is the indicator function $\chi_{\mathcal{K}_1}$ of \mathcal{K}_1 . Then, the dual problem (44) reads

$$\arg \min_{u^* \in L^2(E)} \chi_{\mathcal{K}_1}(u^*) - \frac{1}{2\lambda} [\|u^*\|_{L^2}^2 + 2\langle u^*, \lambda u_0 \rangle_{L^2}] \quad (48)$$

Since the L^2 norm of sections in \mathcal{K}_1 is bounded, it is clear that the functional to minimize in (48) is coercive as well as bounded from below. Then, since $L^2(E)$ is reflexive, we deduce that from any minimizing sequence \underline{u}_n^* for the functional in (48) can be extracted a subsequence $\underline{u}_{n_j}^*$ converging weakly towards some $\underline{u}^* \in L^2(E)$. Finally, as we are in a discrete space, this sequence is actually strongly converging towards \underline{u}^* , showing that \underline{u}^* is a solution of problem (48).

The dual problem can then be rewritten

$$\underline{u}^* = \arg \max_{u^* \in \mathcal{K}_1} \|u^*\|_{L^2}^2 + 2\langle u^*, \lambda u_0 \rangle_{L^2} \quad (49)$$

Adding the term $\|\lambda u_0\|_{L^2}$ does not affect the solution of the problem (49), hence we can write

$$\underline{u}^* = \arg \max_{u^* \in \mathcal{K}_1} \|u^* + \lambda u_0\|_{L^2}^2$$

which is equivalent to

$$\underline{u}^* = -\arg \max_{u^* \in \mathcal{K}_1} \|\lambda u_0 - u^*\|_{L^2}^2$$

Finally, we deduce from (46) and (47) that the solutions \underline{u} of the original problem (41) are

$$\underline{u} = u_0 - \frac{1}{\lambda} \arg \max_{u^* \in \mathcal{K}_1} \|\lambda u_0 - u^*\|_{L^2(E)}^2$$

which can be rewritten

$$\underline{u} = u_0 - \arg \max_{u^* \in \mathcal{K}_{1/\lambda}} \|u_0 - u^*\|_{L^2(E)}^2$$

□

3.2.3. Algorithm to solving the proposed model

As we are in a discrete space, the problem (41) can be rewritten as

$$\arg \min_{u \in L^2 \cap BV_w^{NL}(E)} \frac{\lambda}{2} \|u - u_0\|_{L^2(E)}^2 - \|\nabla_w^{NL} u\|_{L^1} \quad (50)$$

making it be of the form

$$\min_{u \in X} G(u) - F(Au) \quad (51)$$

with $A: X \rightarrow Y$ is a linear operator between two finite dimensional vector spaces, and possessing an adjoint operator A^* .

Then, as demonstrated in [31] and already mentioned in Sect. 3.2.2, the problem (51) has the following dual formulation

$$\min_{u \in X^*} (F \circ A)^*(u) - G^*(u) \quad (52)$$

which is equivalent to

$$\min_{\eta \in Y^*} F^*(\eta) - G^*(A^*\eta) \quad (53)$$

by definition of F .

Hence, the solutions \underline{u} and $\underline{\eta}$ of the primal (51) and dual (53) problems are linked by the following formulae

$$A\underline{u} \in \partial F^*(\underline{\eta}^*) \quad (54)$$

$$A^*\underline{\eta}^* \in \partial G(\underline{u}) \quad (55)$$

Our proposal is then to adapt the Arrow-Hurwicz algorithm (37) to the equations (54) and (55). It gives the following iterative scheme

$$\begin{cases} \eta^{n+1} = \frac{\eta^n + \sigma \nabla_w^{NL} u^n}{\max(1, \|\eta^n + \sigma \nabla_w^{NL} u^n\|_h)} \\ u^{n+1} = \frac{1}{1 + \lambda\tau} [\lambda\tau u_0 + (u_n + \tau \nabla_w^{NL*} \eta^{n+1})] \end{cases} \quad (56)$$

4. Applications to local contrast modification

4.1. The chosen nonlocal covariant derivative and its numerical implementation

4.1.1. The chosen local covariant derivative

Let E be a vector bundle over a Riemannian manifold (M, g) equipped with a positive definite metric h and a covariant derivative ∇ compatible with h . In [4], we showed that the gradient descent of the variational problem

$$\arg \min_u \int_M \|\nabla u\|_{g^{-1} \otimes h}^2 dM \quad (57)$$

is a generalized heat equation

$$\frac{\partial u}{\partial t} + \nabla^* \nabla u = 0 \quad (58)$$

where ∇^* is the adjoint of ∇ .

In [3], Batard and Sochen constructed a covariant derivative ∇^{opt} compatible with a vector bundle metric as solution of a minimization problem, and apply the corresponding heat diffusion (58) for color image regularization purpose.

More precisely, they consider a color image $u = (u^1, u^2, u^3)$ defined on a domain $\Omega \subset \mathbb{R}^2$ as a section of a (trivial) vector bundle E of rank 3 over Ω . Taking the Euclidean scalar product in each fiber as the positive definite metric h on E , they use the fact that a covariant derivative compatible with h is completely determined by a connection 1-form $\omega \in \Gamma(T^*\Omega \otimes \mathfrak{so}(3))$ to construct the desired covariant derivative through a connection 1-form. Then, considering E as an associated bundle $P \times_{(\rho, \text{SO}(3))} \mathbb{R}^3$ where P is the principal bundle $\Omega \times \text{SO}(3)$ over Ω and ρ is the standard representation of $\text{SO}(3)$ on $\text{GL}(\mathbb{R}^3)$, a connection 1-form on E is determined by a horizontal bundle HP on P , which is a subbundle of dimension 2 of P . Finally, they propose a variational model in order to construct an optimal horizontal bundle HP^{opt} of P (see [3] for details). The corresponding optimal connection 1-form ω^{opt} is given by the matrix field coefficients

$$\omega_{12}^{opt} = - \sum_{k=1}^2 \alpha \kappa \left((be-dc)(u_{x_i}^2 u^3 - u_{x_i}^3 u^2) + (bc-ae)(u_{x_i}^1 u^3 - u_{x_i}^3 u^1) + (ad-b^2)(u_{x_i}^1 u^2 - u_{x_i}^2 u^1) \right) dx_i$$

$$\omega_{13}^{opt} = - \sum_{k=1}^2 \alpha \kappa \left((ce-fb)(u_{x_i}^2 u^3 - u_{x_i}^3 u^2) + (af-c^2)(u_{x_i}^1 u^3 - u_{x_i}^3 u^1) + (bc-ae)(u_{x_i}^1 u^2 - u_{x_i}^2 u^1) \right) dx_i$$

$$\omega_{23}^{opt} = - \sum_{k=1}^2 \alpha \kappa \left((fd-e^2)(u_{x_i}^2 u^3 - u_{x_i}^3 u^2) + (ce-fb)(u_{x_i}^1 u^3 - u_{x_i}^3 u^1) + (be-dc)(u_{x_i}^1 u^2 - u_{x_i}^2 u^1) \right) dx_i$$

where

$$\begin{aligned} a &= \delta + \kappa[(u^2)^2 + (u^3)^2] & b &= \kappa u^1 u^2 & c &= -\kappa u^1 u^3 \\ d &= \delta + \kappa[(u^1)^2 + (u^3)^2] & e &= \kappa u^2 u^3 & f &= \delta + \kappa[(u^1)^2 + (u^2)^2] \end{aligned}$$

and

$$\alpha = \frac{1}{2cbe + fad - ae^2 - fb^2 - c^2d}$$

for some $\kappa, \delta > 0$.

Then, they applied the heat diffusion (58) associated to the covariant derivative $\nabla^{opt} = d + \omega^{opt}$ of initial condition the image $u = (u^1, u^2, u^3)$ given in the RGB color space. Moreover, in order to make the diffusion take into account the image edges, they equipped Ω with the following Riemannian metric

$$g: = \begin{pmatrix} 1 + \kappa \sum_{k=1}^3 (u_{x_1}^k)^2 & \kappa \sum_{k=1}^3 u_{x_1}^k u_{x_2}^k \\ \kappa \sum_{k=1}^3 u_{x_1}^k u_{x_2}^k & 1 + \kappa \sum_{k=1}^3 (u_{x_2}^k)^2 \end{pmatrix} \quad (59)$$

in the frame $(\partial/\partial x_1, \partial/\partial x_2)$, where κ is the constant that appears in the expression of ω^{opt} above.

Note that, unlike ∇^{opt} , its adjoint operator ∇^{*opt} depends on g .

Fig. 1 reproduces some of the results available in [3]. It compares the heat diffusion of the operator $\nabla^{opt*} \nabla^{opt}$ to the heat diffusion of the operator $\nabla^{tri*} \nabla^{tri}$ associated to the trivial covariant derivative ∇^{tri} and the Riemannian metric (59), that corresponds to the Laplace-Beltrami operator diffusion introduced in [30]. The same parameters have been taken in both cases, i.e. $\kappa = 0.0005$, $dt = 0.1$, $\delta = 1$, and the diffusions were stopped after 50 iterations. We observe that the heat diffusion based on the optimal covariant derivative preserves more the small details of the original image like the textures and tends also to preserve more its colors.

4.1.2. Nonlocal extension of the chosen covariant derivative

Based on the results obtained in [3] and showed in Fig. 1, we aim at using the optimal covariant derivative ∇^{opt} in the context of the variational models described in this paper. We then need to extend ∇^{opt} in a nonlocal way by the use of the corresponding parallel transport map, as described in Sect. 2.

Numerical computations show that the covariant derivative ∇^{opt} is not flat, meaning that there exist no local frame of E in which its corresponding connection 1-form vanishes, i.e. that there exist no local frame of E in which the parallel transport map associated to ∇^{opt} writes as the Identity map. As a consequence, we have to determine the parallel transport map by solving the following differential equation

$$\nabla_{\dot{\gamma}(t)}^{opt} u(t) = 0, \quad u(0) = u(\gamma(0)) \quad (60)$$

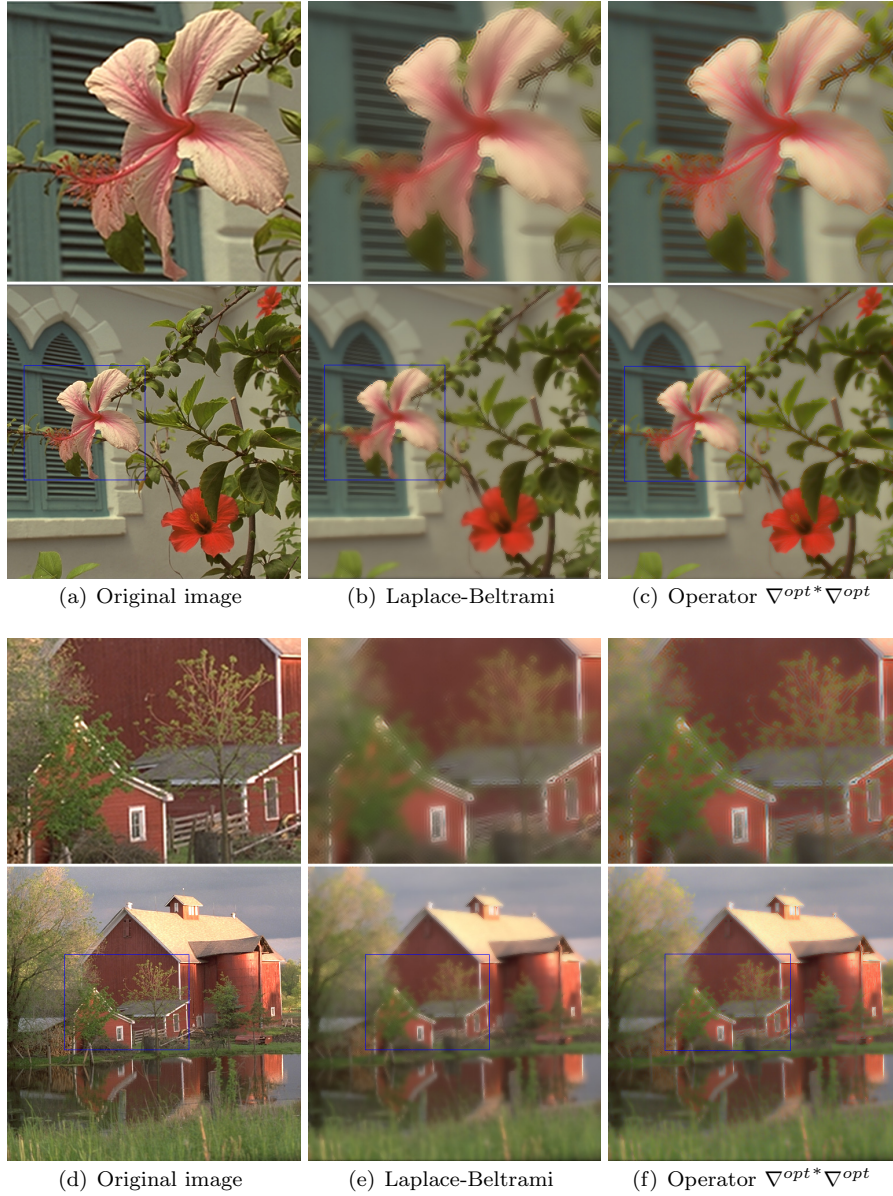


FIG 1. Heat diffusions of generalized Laplacians (58). Comparison between the operator $\nabla^{opt*} \nabla^{opt}$ and the Laplace-Beltrami operator associated to the Riemannian metric (59). Images taken from [3].

i.e.

$$du(t) = -\omega^{opt}(\dot{\gamma}(t))(u(t)), \quad u(0) = u(\gamma(0)) \quad (61)$$

Our proposal is then make us of an explicit Euler scheme

$$u(t_{n+1}) = u(t_n) - dt \omega^{opt}(\dot{\gamma}(t_n))(u(t_n)), \quad u(t_0) = u(\gamma(0)) \quad (62)$$

to solve (61) numerically.

Unlike the local case in Sect. 4.1.1, we equip the image domain Ω with the Euclidean metric in the following experiments where we test the nonlocal models (28) and (41), meaning that the geodesic curves γ in (62) are nothing but the straight lines in Ω . In Sect. 4.1.1, as we were using the L^2 norm of the covariant derivative, we made use of the Riemannian metric (59) in order to guarantee the anisotropy of the diffusion with respect to the edges. In the models (28) and (41), the anisotropy of the diffusion with respect to the edges is taken into account by the L^1 norm of the (nonlocal) covariant derivative.

Finally, we need to determine the symmetric function w in order to complete the construction of the nonlocal covariant derivative (15). The function w completely determines the behavior of the models (28) and (41), meaning that the choice of w is dependent of the application targeted. In this paper, we made the choice of applying the models (28) and (41) to local contrast reduction/enhancement and we then choose w as a truncated (normalized) Gaussian kernel with fixed variance value, but varying the window size.

4.2. Local contrast reduction

In Fig. 2-3, we show the results of our nonlocal regularization model (28) induced by two different covariant derivatives, namely the trivial ∇^{tri} and the optimal ∇^{opt} ones aforementioned, where color images are expressed in the *RGB* color space equipped with the Euclidean metric. Note that the parallel transport map associated to the trivial covariant derivative is nothing but the Identity map. The solutions of both models are computed with the algorithm (37) where we take $\lambda = 0.05$, $\sigma = \tau = 0.1$, and the stopping criteria is

$$\frac{1}{3|\Omega|} \|u_{n+1} - u_n\|_{L^2} < 0.001 \quad (63)$$

Computing the parallel transport map associated to ∇^{opt} through an Euler scheme (62) makes the algorithm (37) be time and memory consumer when the window size of w gets too big, which explains why we only make experiments up to 30×30 window sizes. The variance value we select is 2000, which makes the function w be almost constant.

For both covariant derivatives, we observe on Fig. 2-3 that the window size influences the behavior of the regularizations, i.e. a small window size tends to make the regularization remove the details that were too small in the original images on Fig. 2-3(a) while reducing very few its contrast (Fig. 2-3(b-c)),

whereas a larger window size produces a larger reduction of the contrast of the original images that smoothes the small details but preserves their structure (e.g. textures) (see Fig. 2-3(f-g)), the amount of contrast reduction being correlated with the window size (compare Fig. 2-3(d-e) and Fig. 2-3(f-g)).

Given a window size, the results on Fig. 2-3 confirm what we have observed in [3] with generalized heat diffusions (see Fig. 1), i.e. both covariant derivatives make the model reduce the noise and smooth small details of the original image like its textures, but the optimal covariant derivative makes the model preserve more these small details and produce more saturated colors, meaning that the model preserves more the aspect of the original image than when it is induced by the trivial covariant derivative (compare Fig. 2-3(f) and Fig. 2-3(g)).

In order to measure and compare the amount of contrast reduction of the images on Fig. 2-3(f) and Fig. 2-3(g), we propose to make use of the following mean contrast (MC) measure of their luminances

$$\frac{1}{|\Omega|} \sum_x \sum_y w(x, y) |u_l(x) - u_l(y)| \quad (64)$$

for w being the truncated (normalized) Gaussian kernel of size 30×30 and variance 2000, and where we define the luminance u_l of a color image $u = (u^1, u^2, u^3)$ as $u_l = \frac{1}{3} \sum_{k=1}^3 u^k$.

Fig. 4 shows the luminances of the original color images Fig. 2-3(a) and their contrast reduced versions on Fig. 2-3(f) and Fig. 2-3(g). We compute the mean contrast (64) of each luminance image, and the results show that the reduction of contrast is almost the same for both covariant derivatives.

Finally, through the experiments conducted in this Section, we have shown that using the optimal covariant derivative makes our local contrast reduction model preserve more the aspect of the original image than the trivial covariant derivative does while reducing equally its contrast.

4.3. Local contrast enhancement

In Fig. 5-6, we show the results of our nonlocal enhancement model (41) induced by the optimal and the trivial covariant derivatives aforementioned, where color images are expressed in the RGB color space equipped with the Euclidean metric. The solutions of both models are computed with the algorithm (56) where we take $\lambda = 0.1$, $\sigma = \tau = 0.1$, and the stopping criteria is defined in (63).

Preliminary experiments showed that applying the enhancement model for window sizes and variance values that are too small amplifies the noise of the original images for both the trivial and the optimal covariant derivatives, and the noise amplification tends to reduce with the increase of the window size and the variance value. This is consistent with the results obtained in the previous Section where we showed that the regularization model smoothes the small details of the



(a) Original image u_0



(b) NLCV induced by the trivial one with window size 3×3



(c) NLCV induced by the optimal one with window size 3×3



(d) NLCV induced by the trivial one with window size 10×10



(e) NLCV induced by the optimal one with window size 10×10



(f) NLCV induced by the trivial one with window size 30×30



(g) NLCV induced by the optimal one with window size 30×30

FIG 2. Solutions \underline{u} (29) of the local contrast regularization model (28) for different nonlocal covariant derivatives (NLCV).



(a) Original image u_0



(b) NLCV induced by the trivial one with window size 3×3



(c) NLCV induced by the optimal one with window size 3×3



(d) NLCV induced by the trivial one with window size 10×10



(e) NLCV induced by the optimal one with window size 10×10



(f) NLCV induced by the trivial one with window size 30×30



(g) NLCV induced by the optimal one with window size 30×30

FIG 3. Solutions \underline{u} (29) of the local contrast reduction model (28) for different nonlocal covariant derivatives (NLCV).



FIG 4. Mean Contrast (MC) of luminance images (64). Comparisons between the luminance of original color images (top row) and the luminance of the solutions (29) of the local contrast reduction models (28) for different nonlocal covariant derivative (NLCV).

image besides decreasing its contrast for such window sizes, and the smoothing decreases with the increase of the window size. Hence, we only show on Fig. 5-6 the results where a window size 30×30 and a variance value 2000 have been used, but still we can observe on Fig. 5-6(b-c) some enhancement of the noise, that would not appear using larger window sizes.

Comparing the results obtained with the two different covariant derivatives, we observe that the colors are less saturated in the case of the optimal one (compare Fig. 5-6(b) and Fig. 5-6(c)), making the colors be closer to the ones of the original images and consequently the aspect of the original images be more preserved. This behavior was already observed in the previous Section dealing with local contrast reduction.

A more objective way to determine whether the aspect of the original image has been more preserved using the optimal covariant derivative is to compute how many colors in the contrast enhanced image (Fig. 5-6(b) and Fig. 5-6(c)) belong to the convex hull of the colors of the original image (Fig. 5-6(a)). The black pixels of the images on Fig. 5-6(g-h) represent the colors of Fig. 5-6(b-c) that lie outside the convex hulls of the corresponding original images Fig. 5-6(a), and we see that there are less black pixels on Fig. 5-6(h) than on Fig. 5-6(g), meaning that the contrast enhanced images induced by the optimal covariant derivative on Fig. 5-6(c) have more colors inside the convex hulls of the original images than the ones induced by the trivial covariant derivative on Fig. 5-6(b).

As we did in the previous Section, in order to show that the better preservation of the aspect of the original images using the optimal covariant derivative is not due to the fact that the contrast is less enhanced, we compute and compare the contrast measure (64) of the luminance of the images on Fig. 5-6(b) and Fig. 5-6(c). Results are presented in Fig. 7, and the contrast measure tells us that the model based on the optimal covariant derivative enhances equally (even slightly more) the contrast than the one based on the trivial covariant derivative.

Finally, the experiments on local contrast enhancement that we have conducted in this Section yield the same conclusion as the ones of the previous Section on local contrast reduction, i.e. using the optimal covariant derivative makes the model preserve more the aspect of the original image than the trivial covariant derivative does while enhancing equally its contrast.

4.4. Functional spaces modeling noise, textures and contrast on color images

Given a color image u_0 defined on a discrete grid Ω , we showed in Sect. 3 that the solutions \underline{u} of both models (28) and (41) are of the form

$$\underline{u} = u_0 - u^* \quad (65)$$

where u^* is an element of the space $K_{1/\lambda}$ defined by

$$K_{1/\lambda} := \{\nabla_w^{NL*} \eta : \eta \in \Gamma(pr_1(E)), \|\eta(x, y)\|_{h_x} \leq 1/\lambda \quad \forall x, y \in \Omega\} \quad (66)$$

According to the experiments performed in Sect. 4.2-3 (where the vector bundle metric h has been taken as the Euclidean scalar product in the RGB color space in each fiber, and the function w is a truncated (normalized) Gaussian



(a) Original Image u_0



(b) NLCV induced by the trivial one with window size 30×30



(c) NLCV induced by the optimal one with window size 30×30



(d) Close-up of (a)



(e) Close-up of (b)



(f) Close-up of (c)



(g) 11.72% of the colors of (b) are outside the convex hull of the colors of (a)



(h) 6.46% of the colors of (c) are outside the convex hull of the colors of (a)

FIG 5. (b-c): solutions \underline{u} (42) of the local contrast enhancement model (41) applied to (a) for different nonlocal covariant derivatives (NLCV). Black pixels on (g-h) show the colors of (b-c) that lie outside the convex hull of the colors of (a).



(a) Original Image u_0



(b) NLCV induced by the trivial one with window size 30×30



(c) NLCV induced by the optimal one with window size 30×30



(d) Close-up of (a)



(e) Close-up of (b)



(f) Close-up of (c)



(g) 3.79% of the colors of (b) are outside the convex hull of the colors of (a)



(h) 1.98% of the colors of (c) are outside the convex hull of the colors of (a)

FIG 6. (b-c): solutions \underline{u} (42) of the local contrast enhancement model (41) applied to (a) for different nonlocal covariant derivatives (NLCV). Black pixels on (g-h) show the colors of (b-c) that lie outside the convex hull of the colors of (a).



FIG 7. Mean Contrast (MC) of luminance images (64). Comparisons between the luminance of original color images (top row) and the luminance of the solutions (42) of the local contrast reduction models (41) for different nonlocal covariant derivative (NLCV).

kernel), these variational models reduce or enhance the local contrast of the original image u_0 , the parameter λ being inversely proportional to the intensity of the reduction or enhancement of the local contrast, and the window size determines the features involved: a very small window size makes the variational models affect mainly the noise and the small details of the image like its textures

and very few its contrast, whereas a larger window size makes the variational models affect mainly the contrast of the image. We can then deduce that the spaces $K_{1/\lambda}$ (associated to the trivial and optimal covariant derivatives aforementioned), model noise, textures and contrast of color images.

It is also worth noting that, in the scalar case and when the covariant derivative is the trivial one, reducing the window size makes the local contrast reduction model tend towards the ROF model [28] which aims at removing the noise on gray-level images, but has tendency to remove the textures and reduce (slightly) the contrast, and this is consistent with the experiments in Sect. 4.2 (see Fig. 2-3(b-c)). Let us also point out that reducing the window size makes the space $K_{1/\lambda}$ tend towards the space

$$\{\nabla^* \eta: \eta \in C^\infty(\Omega; \mathbb{R}^2), |\eta(x)| \leq 1/\lambda \ \forall x \in \Omega\}, \quad (67)$$

where ∇^* is the adjoint of the Euclidean gradient operator, which is a subspace of the space of oscillating patterns introduced by Meyer [24]. Oscillating patterns can then be considered as a limit of local contrast when reducing the size of the neighborhood.

On Fig. 8-9, we show the results of the differences between the solutions of both variational models (28) and (41) applied to the same original image u_0 and the original image itself, i.e. we show the element u^* in (65), which is given by

$$u^* = \arg \min_{v \in K_{1/\lambda}} \|u_0 - v\|_{L^2}^2, \quad (68)$$

in the local contrast reduction model (see Fig. 8), and by

$$u^* = \arg \max_{v \in K_{1/\lambda}} \|u_0 - v\|_{L^2}^2, \quad (69)$$

in the local contrast enhancement model (see Fig. 9).

We test both models with the two covariant derivatives aforementioned and two different window sizes, i.e. 10×10 and 30×30 . Moreover, we use the same parameter value $\lambda = 0.1$ and stopping criteria (63).

Through the observation of the positive and negative parts of u^* and the comparisons between the two different window sizes, we deduce a region-wise oscillating behavior of u^* around the value 0, that tends to get pixel-wise when reducing the window size. We also observe color oscillations of smaller saturation in the case of the optimal covariant derivative, which explains why this covariant derivative makes the regularization and enhancement models preserve more the colors of the original image. Finally, a comparison between the results on Fig. 8 and Fig. 9 reveals big similarities in the case of the window size 30×30 between the positive part of the local contrast reduction model and the negative part of the local contrast enhancement model and vice-versa, meaning that the elements u^* are close to be opposite. This result is consistent with the expressions of u^* in (68) and (69) and the fact that $K_{1/\lambda}$ is the image of a ball through a linear

map. However, the similarities are much less obvious for the smaller window size 10×10 due to the large noise amplification of the local contrast enhancement model.

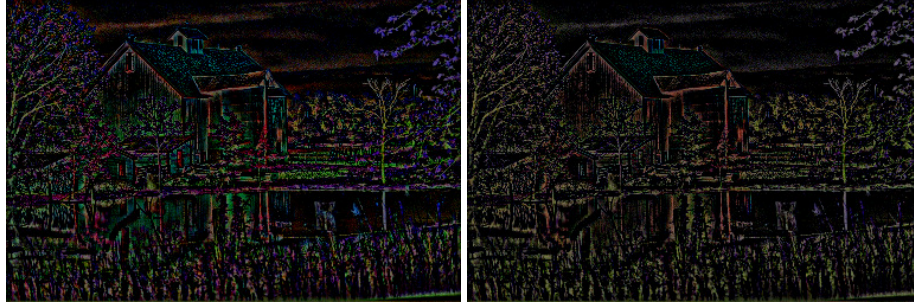
5. Conclusion and further work

We have introduced the notion of nonlocal covariant derivative on a vector bundle from which we have derived the concept of nonlocal total variation for sections of a vector bundle. We have then provided an application of these new mathematical tools to image processing by extending existing variational models devoted to local contrast reduction/enhancement from the Euclidean space to a vector bundle. For a well-chosen nonlocal covariant derivative, we have shown that the models preserve more the aspect of the original image than the existing Euclidean models do, while reducing/enhancing equally its contrast. As contrast reduction/enhancement is deeply related with human vision and covariant differentiation models some properties of the human visual system too, we are investigating the relations between the proposed mathematical model and human vision.

However, the current algorithm is rather slow, mainly due to the fact that the nonlocal covariant derivative between two points is the solution of an ODE, whose explicit solution is unknown, and has then to be solved through a numerical scheme. This computational issue forces us to deal with small window sizes and it makes the models act on noise and textures while modifying the image contrast, which can be undesirable in some applications where contrast reduction/enhancement is useful. Current work is then devoted to speeding up the algorithm in order to make it applicable on large window sizes.

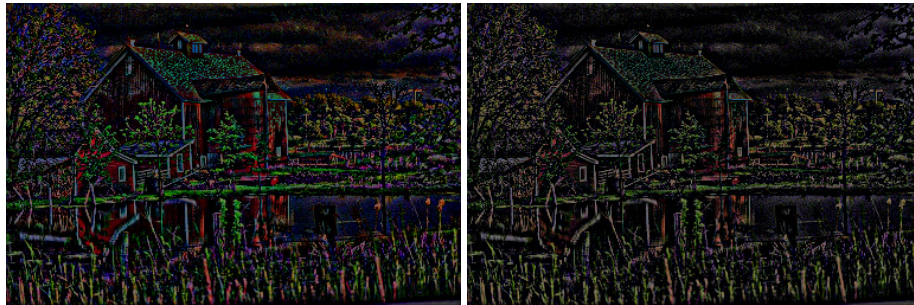
References

- [1] AWATE, S.P., WHITAKER, R.T. (2006) Unsupervised, information-theoretic, adaptive image filtering for image restoration. *IEEE Trans. Pattern Anal. Mach. Intell.* **28(3)** 364–376
- [2] BATARD, T. (2011) Heat equations on vector bundles - application to color image regularization. *J. Math. Imaging Vis.* **41(1-2)** 59–85
- [3] BATARD, T., SOCHEN, N. (2014) A class of generalized Laplacians devoted to multi-channels image processing. *J. Math. Imaging Vis.* **48(3)** 517–543
- [4] BATARD, T., BERTALMÍO, M. (2014). On covariant derivatives and their applications to image regularization. *SIAM J. Imaging Sci.* **7(4)** 2393–2422
- [5] BATARD, T., BERTALMÍO, M. (2015). Duality principle for image regularization and perceptual color correction models. *Lecture Notes in Computer Science, Springer.* **9087** 449–460
- [6] BERTALMÍO, M. (2014). *Image Processing for Cinema*. Chapman & Hall/CRC
- [7] BERTALMÍO, M., CASELLES, V., PROVENZI, E., RIZZI, A. (2007). Perceptual color correction through variational techniques. *IEEE Trans. Im. Processing* **16(4)** 1058–1072



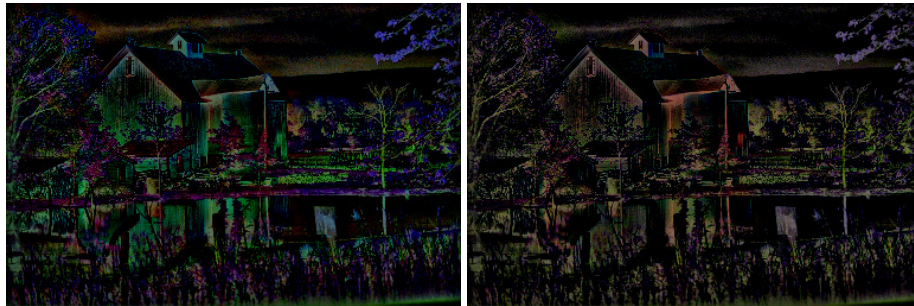
(a) NLCV induced by the trivial one with window size 10×10 : Negative part

(b) NLCV induced by the optimal one with window size 10×10 : Negative part



(c) NLCV induced by the trivial one with window size 10×10 : Positive part

(d) NLCV induced by the optimal one with window size 10×10 : Positive part



(e) NLCV induced by the trivial one with window size 30×30 : Negative part

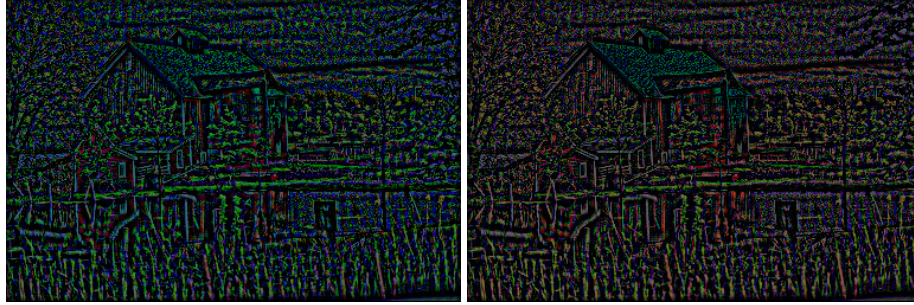
(f) NLCV induced by the optimal one with window size 30×30 : Negative part



(g) NLCV induced by the trivial one with window size 30×30 : Positive part

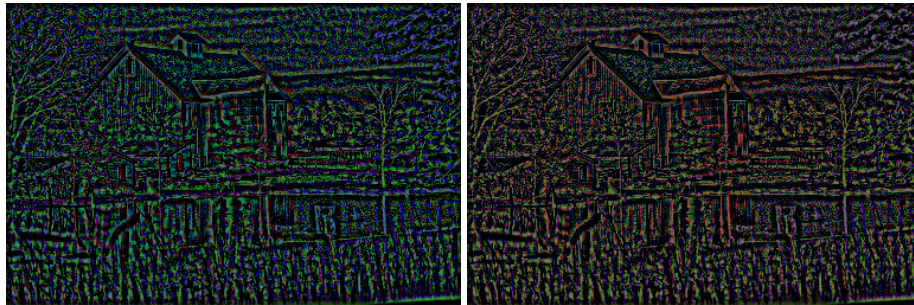
(h) NLCV induced by the optimal one with window size 30×30 : Positive part

FIG 8. Difference $u^* = u_0 - \underline{u}$ (68) for the local contrast reduction model with different nonlocal covariant derivatives (NLCV) applied to u_0 on Fig. 2(a). Values multiplied by 10 for visualization purposes.



(a) NLCV induced by the trivial one with window size 10×10 : Negative part

(b) NLCV induced by the optimal one with window size 10×10 : Negative part



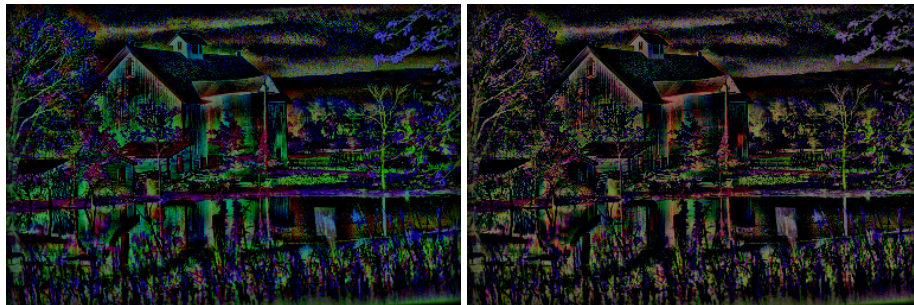
(c) NLCV induced by the trivial one with window size 10×10 : Positive part

(d) NLCV induced by the optimal one with window size 10×10 : Positive part



(e) NLCV induced by the trivial one with window size 30×30 : Positive part

(f) NLCV induced by the optimal one with window size 30×30 : Positive part



(g) NLCV induced by the trivial one with window size 30×30 : Positive part

(h) NLCV induced by the optimal one with window size 30×30 : Positive part

FIG 9. Difference $u^* = u_0 - \underline{u}$ (69) for the local contrast reduction model with different nonlocal covariant derivatives (NLCV) applied to u_0 on Fig. 2(a). Values multiplied by 10 for visualization purposes.

- [8] BERTALMÍO, M., CASELLES, V., PROVENZI, E. (2009) Issues about Retinex theory and contrast enhancement. *Int. J. Computer Vis.* **83** 101–119
- [9] BERTALMÍO, M., COWAN, J.D. (2009) Implementing the Retinex algorithm with Wilson-Cowan equations. *J. Physiology* **103** 69–72
- [10] BREDIES, K., KUNISH, K., POCK, T. (2010). Total generalized variation. *SIAM J. Imaging Sci.* **3(3)** 492–526
- [11] BRESSON, X., CHAN, T. F. (2008). Fast dual minimization of the vectorial total variation norm and applications to color image processing. *Inverse Probl. Imaging* **2(4)** 455–484
- [12] BUADES, A., COLL, B., MOREL, J.-M. (2005) A non-local algorithm for image denoising. *Proceedings of CVPR* **(2)** 60–65
- [13] CHAMBOLLE, A. (2004) An algorithm for total variation minimization and applications. *J. Math. Imaging Vis.* **20(1-2)** 89–97
- [14] CHAMBOLLE, A., POCK, T. (2011) A first-order primal-dual algorithm for convex problems with applications to imaging. *J. Math. Imaging Vis.* **40(1)** 120–145
- [15] FERRADANS, S., BERTALMÍO, M., PROVENZI, E., CASELLES, V. (2011) An analysis of visual adaptation and contrast perception for tone mapping. *IEEE Trans. Pattern Anal. Mach. Intell.* **33(10)** 2002–2012
- [16] FITSCHEN, J.H., NIKOLOVA, M., PIERRE, F., STEIDL, G. (2015) A variational model for color assignment. *Lecture Notes in Computer Science, Springer* **9087** 437–448
- [17] FRANKEN, E., DUITZ, R. (2009) Crossing-preserving coherence-enhancing diffusion on invertible orientation scores. *Int. J. Computer Vis.* **85** 253–278
- [18] GALDRAN, A., VAZQUEZ-CORRAL, J., PARDO, D., BERTALMÍO, M. Enhanced variational image dehazing. *To appear in SIAM J. Imaging Sci.*
- [19] GILBOA, G., OSHER, S. (2008) Nonlocal operators with applications to image processing. *Multiscale Model. Simul.* **7(3)** 1005–1028
- [20] GOLDLUECKE, B., STREKALOVSKIY, E., CREMERS, D. (2012) The natural vectorial total variation which arises from geometric measure theory. *SIAM J. Imaging Sci.* **5** 537–563
- [21] JIN, Y., JOST, J., WANG, G. (2014) A new nonlocal H^1 model for image denoising. *J. Math. Imaging Vis.* **48(1)** 93–105
- [22] KINDERMANN, S., OSHER, S., JONES, P.W. (2005) Deblurring and denoising of images by nonlocal functionals. *Multiscale Model. Simul.* **4(4)** 1091–1115
- [23] LAWSON, H. B., MICHELSON, M.-L. (1989). *Spin Geometry*. Princeton University Press.
- [24] MEYER, Y. (2001) Oscillating patterns in image processing and in some nonlinear evolution equations. *The Fifteenth Dean Jacqueline B. Lewis Memorial Lectures*.
- [25] PALMA-AMESTOY, R., PROVENZI, E., BERTALMÍO, M., CASELLES, V. (2009) A perceptually inspired variational framework for color enhancement. *IEEE Trans. Pattern Anal. Mach. Intell.* **31(3)** 458–474
- [26] PEDERSEN, M., HARDEBERG, J. (2011) Full-reference image quality met-

- rics: classification and evaluation. *Found. Trends Comp. Graphics and Vision* **7** 1-80
- [27] ROCKAFELLAR, R. T. (1970) *Convex Analysis*. Princeton University Press
- [28] RUDIN, L.I., OSHER, S., FATEMI, E. (1992) Nonlinear total variation based noise removal algorithms. *Physica D* **60** 259–268
- [29] SAPIRO, G., CASELLES, V. (1997) Histogram modification via differential equations. *J. Differential Equations* **135** 238–268
- [30] SOCHEN, N., KIMMEL, R., MALLADI, R. (1998) A general framework for low level vision. *IEEE Trans. Im. Processing* **7** 310–318
- [31] TOLAN, J.F. (1979) A duality principle for non-convex optimisation and the calculus of variations. *Archiv. Rational Mech. Analysis* **71(1)** 41–61
- [32] WANG, Z., BOVIK, A. (2002) A universal image quality index. *IEEE Signal Process. Letters* **9(3)** 81–84
- [33] ZOSSO, D., TRAN, G., OSHER, S. (2015) Non-local Retinex — A unifying framework and beyond. *SIAM J. Imaging Sci.* **8(2)** 787–826
- [34] WEICKERT, J. (1999) Coherence-enhancing diffusion of color images. *Im. Vis. Computing* **17** 201–212
- [35] ZAMIR, S. W., VAZQUEZ-CORRAL, J., BERTALMIÓ, M. (2014) Gamut mapping in cinematography through perceptually-based contrast modification. *IEEE J. Sel. Topics Signal Processing* **8(3)** 490–503
- [36] ZHU, W., CHAN, T. (2012) Image denoising using mean curvature of image surface. *SIAM J. Imaging Sci.* **5** 1–32

Department of Information and Communication Technologies,
University Pompeu Fabra, Barcelona (Spain)
e-mail: thomas.batard@upf.edu

Department of Information and Communication Technologies,
University Pompeu Fabra, Barcelona (Spain)
e-mail: marcelo.bertalmio@upf.edu